Research Article

Tharaka Kaushalya, Markus Littow, Eetu Virta, Tarmo Ruotsalainen, Jari Juuti, Yang Bai*

A system-level study of indoor light energy harvesting integrating commercially available power management circuitry

https://doi.org/10.1515/EHS-2023-0164
received November 24, 2023; accepted April 20, 2024

Abstract: With the development of sustainable and energy-efficient buildings and cities, scavenging indoor light energy to power Internet of Things has become an increasingly attractive solution. However, the energy that can be harvested from an indoor light environment is limited compared to natural, outdoor sunlight, emphasizing the importance of efficiency of the entire energy harvesting system rather than that of individual harvesters. Power management circuitry plays a crucial role here but there has not been a system-level study for different power management schemes when connected to both harvesters and batteries whilst working under real lighting conditions. This study evaluates four integrated indoor light energy harvesting systems containing two distinctive types of photovoltaic cells connected to a switched capacitor (SC) and an inductor-based (IN) boost converter, respectively, as well as a Li-ion battery. Charging efficiencies of the entire systems, in addition to those of individual components, are assessed. Results suggest that for an indoor light energy harvesting system, although the IN converter tends to be cumbersome, it provides unbeatably high and stable battery charging efficiency across a broad range of light intensities compared to the SC converter even though the latter is specifically designed for low-power applications competing with the IN counterpart.

Keywords: energy harvesting, sensing, indoor light, Li-ion battery, photovoltaic, smart building

*** Corresponding author: Yang Bai,** Microelectronics Research Unit, Faculty of Information Technology and Electrical Engineering, University of Oulu, FI-90570, Oulu, Finland, e-mail: yang.bai@oulu.fi
Tharaka Kaushalya: Microelectronics Research Unit, Faculty of Information Technology and Electrical Engineering, University of Oulu, FI-90570, Oulu, Finland; Nordic Semiconductor Oy, Yrttipellontie 1D, FI-90230, Oulu, Finland, e-mail: tharaka.salamanarachchigedon@oulu.fi
Markus Littow: Nordic Semiconductor Oy, Yrttipellontie 1D, FI-90230, Oulu, Finland, e-mail: markus.littow@nordicsemi.no
Eetu Virta: Microelectronics Research Unit, Faculty of Information Technology and Electrical Engineering, University of Oulu, FI-90570, Oulu, Finland, e-mail: eetu.parkkinen@oulu.fi
Tarmo Ruotsalainen: Nordic Semiconductor Oy, Yrttipellontie 1D, FI-90230, Oulu, Finland, e-mail: tarmo.ruotsalainen@nordicsemi.no
Jari Juuti: Microelectronics Research Unit, Faculty of Information Technology and Electrical Engineering, University of Oulu, FI-90570, Oulu, Finland, e-mail: jari.juuti@oulu.fi

1 Introduction

1.1 Internet of Things (IoT) and energy harvesting

The IoT is reshaping our lives by making things more autonomous, accessible, secure, and productive. With the advent of ubiquitous wireless sensing and communication networks, billions of IoT devices are expected to be distributed in our living environment to gather and share data through the internet, especially thanks to the rapid development of 4G and 5G telecommunication technologies (Zanella et al. 2014, Masek et al. 2018). For instance, the long-term evolution machine type communication (LTE-M) and narrowband IoT standards defined in the 4G era have induced the massive deployment of IoT devices nowadays. Perpetual and autonomous operation with minimal need for on-site maintenance is a crucial factor to ensure a successful application of any IoT device (Lin et al. 2017, Zeadally et al. 2020). However, the limited capacity of the finite power source is considered one of the bottlenecks here. In the current IoT architectures, batteries are the most likely power sources. Yet, the power requirements for IoT devices are increasing drastically due to boosted functionalities, resulting in a battery lifespan of a few years maximum without recharging or replacement (Akan et al. 2018, Bai et al. 2018), while an IoT device is expected to be able to operate for 10–20 years without service interruption. A viable option to meet such a power demand is to improve the battery lifespan via smart energy management schemes while introducing energy harvesting technology.

Energy harvesters scavenge ambient energy sources that would be wasted if not harvested, from the devices' working environments (Bai et al. 2018). Ambient light, for instance, can be a good candidate to be harvested and then used to power wireless sensing systems integrated into smart buildings (Al-Obaidi et al. 2022). Using indoor artificial light to charge the batteries and thus to greatly extend the lifespan of the power source is becoming popular in IoT nodes used in smart buildings (Yue et al. 2017).

1.2 Challenge for indoor light energy harvesting systems

Compared to outdoor solar energy harvesting, indoor light harvesting faces a significant challenge that is the much smaller and highly intermittent input energy flow. The solar energy received by outdoor solar panels can be as high as 10^5 lux. Meanwhile, although being affected by weather conditions, variation in solar energy to be harvested by outdoor solar panels is gentle and predictable within each hour, or even over the course of a day. In comparison, indoor artificial light sources can only provide up to 10^3 lux and indoor light can also be interrupted minute by minute in practical scenarios (Kozalakis et al. 2021). This is because indoor light energy harvesters are usually fitted with the IoT devices to be powered and thus the power is produced on-site. Users and other moving objects may cause intermittent shadows, for instance, when the IoT device is a wearable or is installed in a public space with a constant flow of people. Some modern office buildings have smart switches fitted to lamps so that lights will be turned off automatically when not in use. In addition, because of the on-site power generation, the size of the photovoltaic (PV) cells used for indoor light energy harvesting is limited to only a few square centimeters for each device, leading to a low input power level of less than 100 μW (Kozalakis et al. 2021, Yu and Yue 2012). While for outdoor energy production, the area of the solar panel is not strictly constrained, and the power does not need to be generated on-site where it is to be used. The electricity can be generated at an energy-abundant location and then transported to the users at another location. Therefore, indoor light exhibits a more dynamic feature than that of solar energy.

Making use of such a low-level of power demands intelligent ultralow power management integrated circuits (PMICs) to complete the necessary DC–DC boost conversion, so that the harvested power can effectively charge an energy storage element. There are several high-efficiency energy harvesting converter designs proposed in the literature. For instance, Yu et al. (2015) reported an inductor-based (IN) DC–DC buck boost converter PMIC which can convert harvested indoor light energy with an efficiency of 83% with low quiescent current requirements. Qiu et al. (2011) also proposed an IN boost converter PMIC which can regulate the optimum power point of a photovoltaic (PV) cell over a broad input power range of 5 μW–10 mW to charge a battery with an efficiency of 87%. Lee et al. (2016) designed a fully integrated PMIC with a switched capacitor (SC)-based boost conversion mechanism, instead of the IN, to harvest light intensities from 10^2 to 10^5 lux while charging a 1.5–2.5 V battery with a 78% efficiency. Jung et al. (2014) published a fully integrated SC DC–DC converter PMIC specifically for indoor light harvesting under very low illumination levels, tailored for form-factor constrained applications.

There are also several commercial products integrated with PMICs available for solar or indoor light energy harvesting, including the electronic shelf label system (Nexperia 2023), the energy autonomous Nordic Thingy 91 module (Nordic Semiconductor 2021), the SODAQ asset tracker (SODAQ 2023), and the Telink TV remote control (Telink 2023).

1.3 Two major working mechanisms of PMIC

PMICs are designed to efficiently regulate and manage power, including the tasks of voltage regulation, current control, power conversion, and battery management. For indoor light energy harvesting systems, the PMIC should enable real-time control of varying voltage levels and thus minimization of energy loss. It should also prevent energy storage from being overcharged by providing feedback on system status. Two main types of PMIC architectures are used for indoor light energy harvesting systems, as shown in Figure 1.

Figure 1(a) explains a single-stage voltage doubler where two pairs of switches operate alternatively while each pair opens and closes synchronously. When both $S_{1\text{-}a}$ are closed and both $S_{2\text{-}a}$ are open, $C_{1\text{-}a}$ is charged to the input voltage ($V_{in\text{-}a}$), then both $S_{2\text{-}a}$ are closed and both $S_{1\text{-}a}$ are opened, putting $C_{1\text{-}a}$ in series connection with $V_{in\text{-}a}$, which doubles the output voltage ($V_{out\text{-}a}$) (Forouzesh et al. 2017). In this architecture, the peak voltage conversion efficiency is achieved when the actual voltage ratio of $V_{out\text{-}a}$ to $V_{in\text{-}a}$ is approximately 2:1. When this ratio deviates, $C_{1\text{-}a}$ undergoes charge and discharge cycles, leading to an increase in loss caused by charge redistribution and hence unnecessary energy loss which ultimately reduces the energy conversion efficiency. In practice, multiple single-stage voltage doublers are cascaded, and the voltage ratios are dynamically adjusted. An optimum voltage ratio that always matches the real-time ratio is a crucial factor for efficient boost conversion (Yoon et al. 2022).

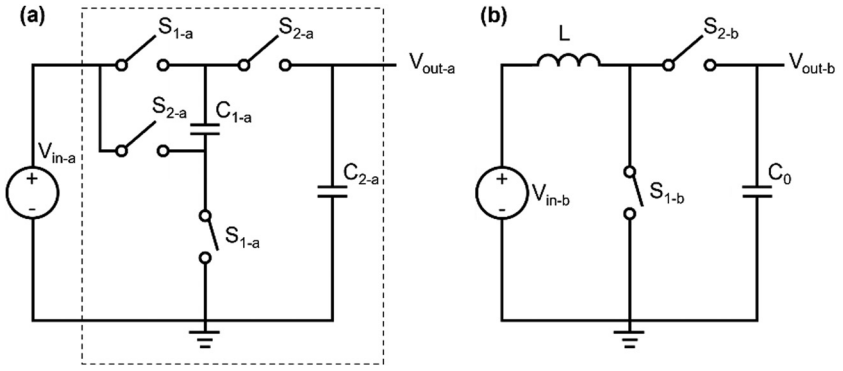

Figure 1: Schematics of (a) SC and (b) IN boost converter circuits.

Figure 1(b) demonstrates boost conversion through an inductive element (L), where two switches operate alternatively. When $S_{1\text{-}b}$ is closed and $S_{2\text{-}b}$ is open, current flows through L and generates a magnetic field which stores energy in L. When $S_{1\text{-}b}$ is open and $S_{2\text{-}b}$ is closed, the magnetic field releases through a voltage which is additive to $V_{in\text{-}b}$, resulting in an increased $V_{out\text{-}b}$. Since L is continuously transferring energy between the input and output ends, $V_{out\text{-}b}$, i.e., the accumulated voltage across C_0, keeps increasing. This mechanism allows $V_{out\text{-}b}$ to eventually become higher than $V_{in\text{-}b}$. By adjusting the duty cycle of the switches, the converter may regulate $V_{out\text{-}b}$ to be at the desired level. The value of the inductance significantly influences energy storage and release rates. A larger inductance induces a larger energy storage capacity but can lead to slower voltage adjustment while a smaller inductance enables faster voltage adjustment but compromises on energy storage capacity. In addition, the switching frequency is also vital, with a higher frequency facilitating faster energy transfer but leading to increased loss. Balancing the inductance and switching frequency is critical for the optimization of IN boost converter.

1.4 Rationale of this work

In general, the IN boost converter tends to be bulky due to the inevitably large physical size of the inductor. Historically, IN boost converters have been mainly used for high-power (>100 mW) applications while SC boost converters have been limited to low-power (<100 mW) applications (Seeman et al. 2010). Previous study has also reported that SC boost converters can also become promising for high-power applications with advantages in terms of switch utilization, reactive utilization, and integration (Seeman et al. 2010). Nowadays, when the power management task also needs to be applied to ultralow-power (<1 mW) applications as is the case for indoor light energy harvesting, default options have still been SC and IN boost converters.

Nevertheless, due to the limited number of options for commercially available PV, power management and energy storage components that can be used to build the systems, one cannot assume the SC option to be more advantageous than the IN counterpart, and the knowledge gap here is that no study has focused on comparing SC and IN boost converters for indoor light energy harvesting applications on a system level. A standalone high-performance PMIC may not be blindly matched with any individual high-performance indoor light harvester. This is because there are many key features in PMICs which determine the overall efficiency of the entire energy harvesting system, including high boost conversion efficiency, maximum power point tracking (MPPT), overcharge and over-discharge protection, low voltage start-up, and lowest footprint with fewest passive components (Chong et al. 2019). An inappropriate matching due to varying input-output conditions between an individual high-performance PMIC and a high-performance harvester may surprisingly lead to a low overall energy harvesting capability for the entire system. A key challenge in successfully pairing PMICs and harvesters is accounting for the fluctuating input light source and real-time battery voltage during charging.

Hence, this study evaluates the charging efficiency of batteries connected to distinct types of commercially available PMICs and harvesters tested under various lighting conditions. Results suggest that combination of the better-performing individual harvesting, power management, and storage component options does not necessarily give a better system-level performance. However, in practice, it is the system-level performance matters rather than that of discrete components. The work provides insights into the selection criteria of PMICs in consideration of the energy harvesters to be connected in practical use cases. It also suggests a solution for making self-sufficient IoT systems under indoor light. In particular, despite the fact that the

IN PMIC tends to be bulky, its performance seems to be unbeatable by the SC PMIC in terms of battery charging efficiency. Efficiency is a brutal criterion of judgement for practical applications of ultralow-power indoor light energy harvesting.

1.5 Structure of this study

Section 2 elaborates the reason and method of selecting the commercial PMIC and PV cell components in this work. It should be noted that the comparisons made for the PMIC and PV cells are not to judge their individual performances but rather to provide key specifications that are carefully considered in order to build a compatible energy harvesting system using these components. Other available options may perform better but are not necessarily compatible with the low intensity of indoor light as the input energy to the system. The testing method is also described in Section 2.

Section 3 comprehensively shows the testing results and thus indicates the fact of how and why combination of better-performing individual components may not necessarily induce a better system-level performance. It also suggests what kind of integration can achieve a fully self-sufficient IoT sensing system under ambient indoor light.

Section 4 provides energy harvesting designers with crucial criteria when considering building a commercially viable indoor light energy harvesting system. Section 5 concludes this work and gives perspective for possible further developments.

2 Methodology

2.1 Selection of the PMICs

Indoor light sources provide an intermittent and irregular supply of energy in practice. For this reason, the PMIC used to manage the harvested energy to charge the energy storage should be intelligently adaptive to dynamic ambient conditions and have a low power consumption. Although there are several energy harvesting chips in the market, selection of the right chip can be a challenging task since it is mostly application specific. A number of key specifications need to be considered carefully.

In this study, two commercially available PMICs for energy harvesting purposes were selected for evaluation. They operate on the SC and IN topologies, respectively, as has been introduced in Section 1. The SC integrated circuit (IC-1) was designed to extract power from indoor light (DC signals) and vibrations (AC signals) for charging batteries or supercapacitors. It is known for its very low assembly footprint, which is beneficial for applications with space constraints. The IN integrated circuit (IC-2) was designed to receive only DC power from PV cells efficiently for charging batteries and supercapacitors. It has an integrated ultralow-power boost converter as well as an efficient low drop-out voltage regulator to drive low-power wireless applications. The key parameters of IC-1 and IC-2 are listed in Table 1.

It should be particularly noted that the comparison in Table 1 was not made to judge the performance of the two products. It rather presents the absolute limits of each PMIC as defined by their datasheets. These specifications were fixed and inherent to each PMIC, serving as fundamental parameters guiding the analysis of their performance under various conditions.

For instance, the input power range for IC-1 was specified as 10 µW–2 mW, while for IC-2, it was 3 µW–550 mW. The input voltage range for IC-1 spanned from 300 mV to 5 V, while for IC-2, it ranged from 50 mV to 5 V. These values highlight the absolute operational limits of each PMIC rather than the conditions under which they were tested. In this work, common ranges for the input operating conditions were chosen to match the voltage and power ranges of other integrated components in the systems to be tested, including (1) Li-ion battery as the energy storage component which could operate within the typical range of 3–4.2 V, aligning well with the output voltage range of the PMICs and (2) PV cells that were specifically designed for indoor lighting conditions as the energy harvesting component, selected based on their open-circuit voltage ranging from 2 to 3.8 V and maximum power levels ranging from 23

Table 1: Comparison of key specifications of the chosen PMICs in this work

	IC-1	IC-2
Supplier	Nowi	E-peas semiconductors
Model	NH2D0245	AEM10941
Input power	10 µW–2 mW	3 µW–550 mW
Input voltage	300 mV–5 V	50 mV–5 V
Output voltage	2.5–5 V	1.2–4.5 V
MPPT algorithm	Hill climbing	Open-circuit voltage based
Quiescent current	625 nA	450 nA
Efficiency	60–80%	70–95%
Topology	SC	IN
Area	12 mm^2	25 mm^2

to 609 μW, as is given in Table 2. These values overlap the input range of the chosen PMICs, ensuring a fair evaluation in this work.

It is admitted that finding these two particular commercial PMICs which were suitable for ultralow-power indoor light energy harvesting was not easy. They were selected from all available commercial options for this work by rating and screening the claimed performances on the manufacturers' datasheets while also considering the energy harvesting capabilities of the selected PV cells introduced in Section 2.2.

2.2 Selection of PV cells for indoor light harvesting

Two light harvesters specially made to operate under low-level lighting conditions were selected after a trade-off between the output capabilities of the harvesters and the input capacities of the ICs listed in Table 1. Table 2 summarizes the key parameters of the selected PV cells. Both the cells, i.e., the LAYER OPV (organic PV) cell (Dracula Technologies 2023) (referred as Harvester-1 hereafter) and the PowerFilm LL200-2.4-37 amorphous silicon (a-Si) cell (PowerFilm Solar 2023) (referred as Harvester-2 hereafter), respectively, were purchased. Both of them were designed to be lightweight, flexible indoor modules which can be easily integrated to IoT devices (Mathews et al. 2019).

2.3 Test configuration

Figure 2 illustrates the test configurations used in this work. To analyze the performance of IC-1 and IC-2, corresponding evaluation kits provided by the manufacturers were used. For the individual evaluations of IC-1 and IC-2, the controlled input was provided by a source meter (Model 2450, Keithley, USA) which was directly connected to the input pins of the PMIC (Figure 2(a)). For integrated evaluations of the energy harvesting systems (i.e., PV cell + PMIC), the PV cell under illumination replaced the source meter and was connected to the input pins of the PMIC to provide the input power (Figure 2(b)). A 10 W smart LED bulb (KLL760P-10, UNILUX, France) with adjustable light intensity and color temperature was used as the light source. The preset light intensities were measured and validated with a color spectrometer (RGBW200, ELV, Germany). The color temperature of the input light was fixed at 3,800 K. This color temperature was determined based on the Kruithof curve in which light intensities involved in this work's measurement mostly sit in the "pleasing" region. The output pins of the PMIC were connected to a battery simulator (2281S, Keithley, USA) which mimicked the behavior of a Li-ion battery. The input and output currents and voltages were measured in real time using a DC power analyzer (N6705B, Keysight, USA) where the data were read and processed by a computer. A general outlook of the measurement setup can be seen in Figure 2(c).

In this work, the performance of the PMICs and the energy harvesting systems was quantified by the overall efficiency in the energy harvesting process where the electricity flowed from the harvester to the PMIC and was then transferred to the energy storage element. Such an efficiency (η) is defined by equation (1).

$$\eta = P_o/P_i = (I_o \cdot V_o)/(I_i \cdot V_i), \quad (1)$$

where P_i represents the input power to the PMIC, which is delivered by either the source meter or the PV cell. P_i can be calculated using the input current (I_i) and input voltage (V_i) as measured by the DC power analyzer. P_o denotes the output power of the PMIC, which charges the energy storage. P_o can be determined using the output current (I_o) and output voltage (V_o) measured by the DC power analyzer.

Table 2: Summary of key parameters of the selected PV cells in this work

	Harvester-1	Harvester-2
Model name	LAYER OPV (Dracula Technologies 2023)	LL200-2.4-37 (PowerFilm Solar 2023)
Manufacturer	Dracula Technologies, France	PowerFilm, USA
Technology	Organic PV	Amorphous silicon
Size	64 mm × 69 mm	54 mm × 36.5 mm
Output power	0.52–13.79 μW/cm^2	3.45–22.78 μW/cm^2
Short-circuit current	13–255 μA	43–214 μA
Open-circuit voltage	3–3.8 V	2.4–2.7 V
Input light intensity	50–1,000 lux	200–1,000 lux
Output power range	23–609 μW	68–449 μW

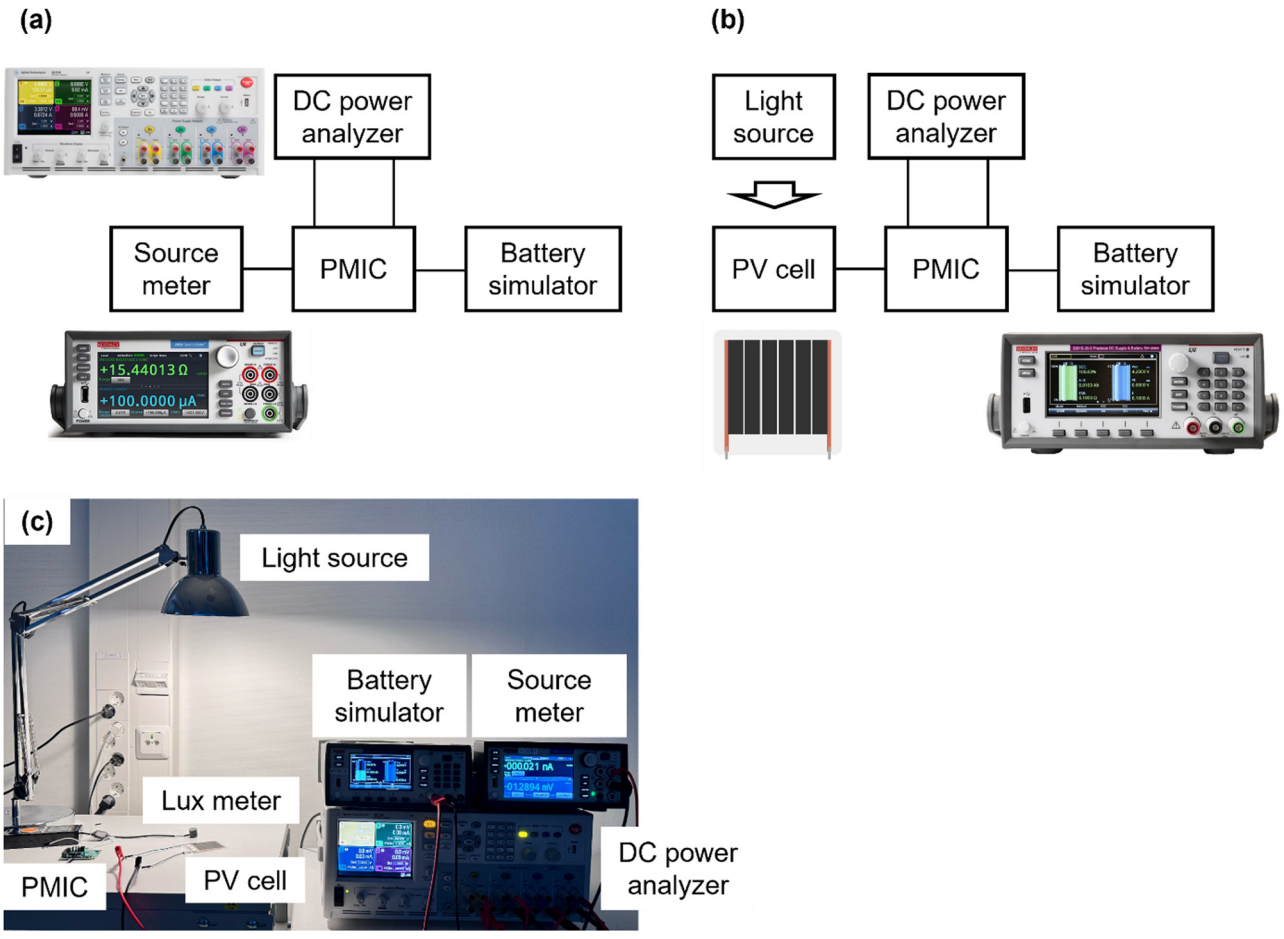

Figure 2: Schematics and pictures of the test configuration. (a) For test methods where the source meter provides the controlled input power; (b) For test methods where the PV cell provides real input power by harvesting indoor light; (c) An overview of the test setup in practice.

2.4 Test methods

This study evaluates η in three ways where two of them used the source meter as the controlled input under simulated ideal conditions. The third method used the PV cells under real indoor lighting conditions as the actual input. Table 3 summarizes the three test methods.

2.4.1 Test method 1 (TM-1)

The battery voltage was controlled by the battery simulator while varying the PMIC's input by means of the source meter. The aim of TM-1 was to examine the performance of the PMICs across the full range of the input specification limits stated in the datasheets at different battery voltages. Here the input current and voltage were adjusted by the source meter and did not violate the maximum ratings of the PMICs as listed in Table 1. Three different battery voltages, 3, 3.7, and 4 V, respectively, were fixed throughout each measurement round. These battery voltages were selected because they are within the vicinity of typical low cut-off, middle plateau, and high cut-off voltages of typical Li-ion batteries. The rationale is that in practice, different IoT devices need to work with different battery

Table 3: Summary of the test methods used for the analyses

Method	Description
TM-1	Analyze η by varying the input power for different battery voltage settings
TM-2	Analyze η across the entire battery voltage range for fixed input power settings
TM-3	Analyze η across a series of indoor light intensities using two different PV cells

voltages and the charging efficiency of the energy harvesting system may be influenced by the battery voltage. Since IC-1 offers two power range settings, namely, high power (HP) and low power (LP) modes, the evaluation was done for both the modes.

2.4.2 Test method 2 (TM-2)

The input was controlled by the source meter while allowing the battery voltage to evolve when subject to charging. The purpose of TM-2 was to investigate the change in η when the battery was being charged from 3 to 4.1 V. Such a voltage range is often used in practice for Li-ion batteries and the relative level of battery voltage can be used to indicate the state of charge (SOC). For instance, in this study, the SOC was considered to increase from 0 to 90% when a typical Li-ion battery is charged from 3 to 4.1 V. The input voltage to the PMICs was fixed at 2.5 V and the input current limit was set to be 1 mA. This setting was determined to ensure that the absolute input power limits of the PMICs would not be violated and the PMIC under test would always boost the voltage from 2.5 V (an approximate medium output voltage value for indoor PV cells). During each measurement round, the battery simulator's model was charged via the PMIC under examination. The corresponding input/output voltage and current were recorded until the battery voltage reached 4.1 V (SOC = 90%).

2.4.3 Test method 3 (TM-3)

The PV cells were used to charge the battery without any active control in the circuitry. The purpose of TM-3 was to evaluate the PMICs' performances in real scenarios. The incident light varied from 75 to 3,500 lux, a range chosen to reflect the recommended indoor lighting conditions for public and private spaces (Brown et al. 2022). Here the PMIC output was connected to the battery simulator and the PMIC input was connected to the PV cell. The average current and voltage were recorded in a 1-min-period for each lux level of the incident light. It should be noted that the above tests were carried out in an air-conditioned laboratory and temperature of the PV cells was verified by a thermocouple to be stable at approximately 21°C throughout the tests.

3 Results

3.1 TM-1

Figures 3 and 4 show the results of TM-1 for IC-1. The η values started to decrease significantly when the input power went up towards 2 mW in the HP mode (Figure 3(a)) and towards 1 mW in the LP mode (Figure 4(a)). Such efficiency drops were expected according to the specifications of the IC-1 listed in Table 1. Here the power modes for the IC-1 are labelled as LP for input power of up to 1 mW and HP for input power of up to 2 mW. In general, the largest η values (>70%) were delivered in the input power range of 40–500 µW for the HP mode and 20–200 µW for the LP mode, respectively. This was also reflected by the input current where the peak input current at maximum efficiency for the HP mode lay at 50 µA (Figure 3(b)) and that for the LP mode was at about 20 µA (Figure 4(b)). It is obvious that the claimed range of η values (60–80%) could be achieved in the input range of

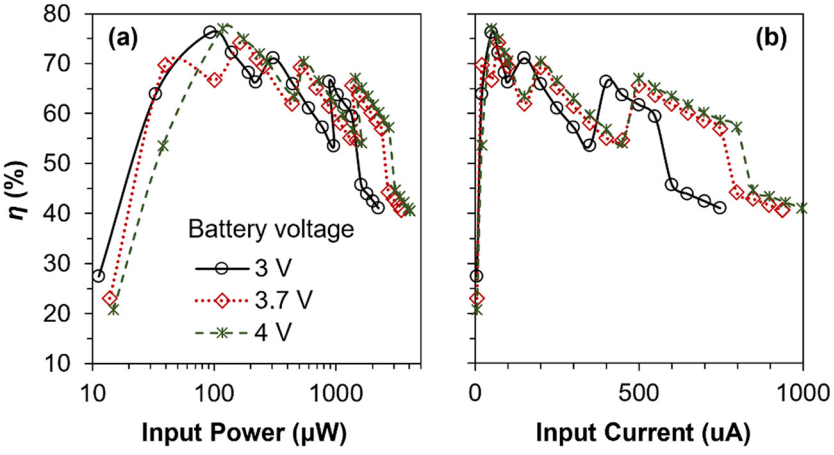

Figure 3: Dependence of η on (a) input power and (b) input current for the IC-1 in HP mode with different battery voltages.

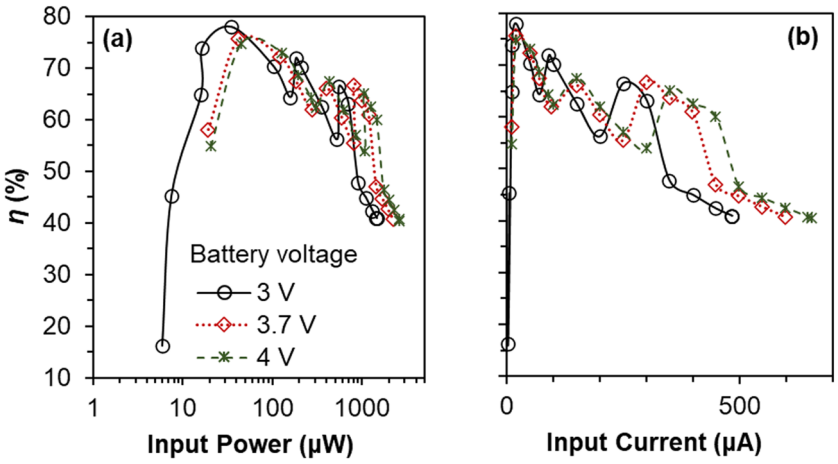

Figure 4: Dependence of η on (a) input power and (b) input current for the IC-1 in LP mode with different battery voltages.

20 μW–2 mW regardless of the power mode, which closely corresponds with the peak efficiency values from manufacturer's data (Table 1).

Figure 5 shows the results of TM-1 for IC-2 where distinctive η values were obtained at different battery voltages. At the battery voltage of 3 V, the charging efficiency was constantly maintained between 70 and 75% throughout the entire input power range (Figure 5(a)), and the same appeared also for the entire input current range (Figure 5(b)). Impressively, the input current range was as wide as several orders of magnitude, spanning from 10 μA to 4 mA. In contrast to IC-2, the efficiencies could become as low as 30–50% for IC-1 when the input power was approaching 10 μW (Figures 3(a) and 4(a)). This implies that IC-2 might be more suitable for charging low-voltage batteries under highly variable lighting conditions, compared to IC-1. For battery voltages of 3.7 and 4 V, IC-2 could still deliver relatively stable η values of around 90% if the input power was above 100 μW. Even though the η values varied significantly at input powers of <100 μW, IC-2 clearly preferred to charge batteries at higher voltage levels with a higher charging efficiency at any input power level (Figure 5(a)). However, this was not the case for IC-1 in the LP mode where the η values at the battery voltage of 3 V (75–80%) were much higher than those at 3.7 or 4 V (55–75%) around the input power of 10 μW (Figure 4(a)). A similar difference could also be seen in the HP mode near 10 μW despite the much smaller η values in general (only 20–30%, Figure 3(a)). For both the HP and LP modes of IC-1, the difference of charging efficiencies caused by battery voltages was not obvious anymore in the input power range of 100 μW–1 mW. The performance of IC-2 in Figure 5 was also consistent with the data in Table 1 (70–95% efficiency).

In summary, the results of TM-1 suggest that, given the same input power settings and the same battery voltages,

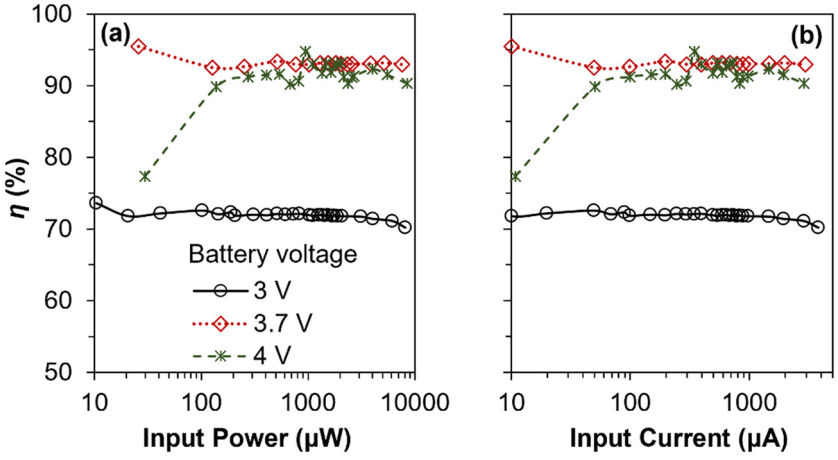

Figure 5: Dependence of η on (a) input power and (b) input current for the IC-2 with different battery voltages.

the efficiency of IC-2 was much higher and more consistent compared to that of the IC-1.

3.2 TM-2

Figure 6 shows the results of TM-2, i.e., the dynamic responses of the charging efficiency with the real-time battery voltage for the IC-1 HP mode, IC-1 LP mode, and the IC-2 were revealed. The raw data directly calculated from equation (1) included unreal spikes caused by instantaneous zero input current during the MPPT actions, as shown in Figure 6(a)–(c). To exclude these artefacts, filtered data are shown in Figure 6(d)–(f).

A linear relationship between the filtered η and the battery voltage was found in both the HP and LP modes for IC-1 (Figure 6(d) and (e)). The boosting conversion was more effective in the HP mode compared to the LP mode where the average η values evolved from 55% to approximately 70% in the HP mode (Figure 6(d)) while the increase was from 50% to only 60% for the LP mode (Figure 6(e)) across the entire battery voltage range (SOC = 0–90%). Since, according to Figures 3 and 4, the battery voltage affected the η values to a less extent compared to that shown in Figure 5, the charging efficiency behaviors for IC-2 were less dynamic and more consistent in real time despite the increased level of efficiency at above 3.5 V battery voltage.

In comparison, IC-2 performed more dynamically compared to IC-1 with the evidence of a jump in the average η values when the battery voltage went beyond 3.6 V (Figure 6(c)). Under 3.6 V, the average charging efficiency was about 70% and at above 3.6 V, the average efficiency was boosted to roughly 90%. This was consistent with that shown in Figure 5. The noticeable jump in efficiency of the IC-2 around 3.6 V can be attributed to the PMIC's internal power mode change as suggested in the datasheet. However, the real-time variation of η values for IC-2 at the battery voltage of >3.6 V (SOC > 57%) was substantial, implying more effort made by the boost converter to achieve a high efficiency at the cost of operational stability.

In summary, the results of TM-2 suggest that, at a given input power setting, the efficiency of IC-2 remained much higher than that of IC-1 across the entire operation voltage range of the battery.

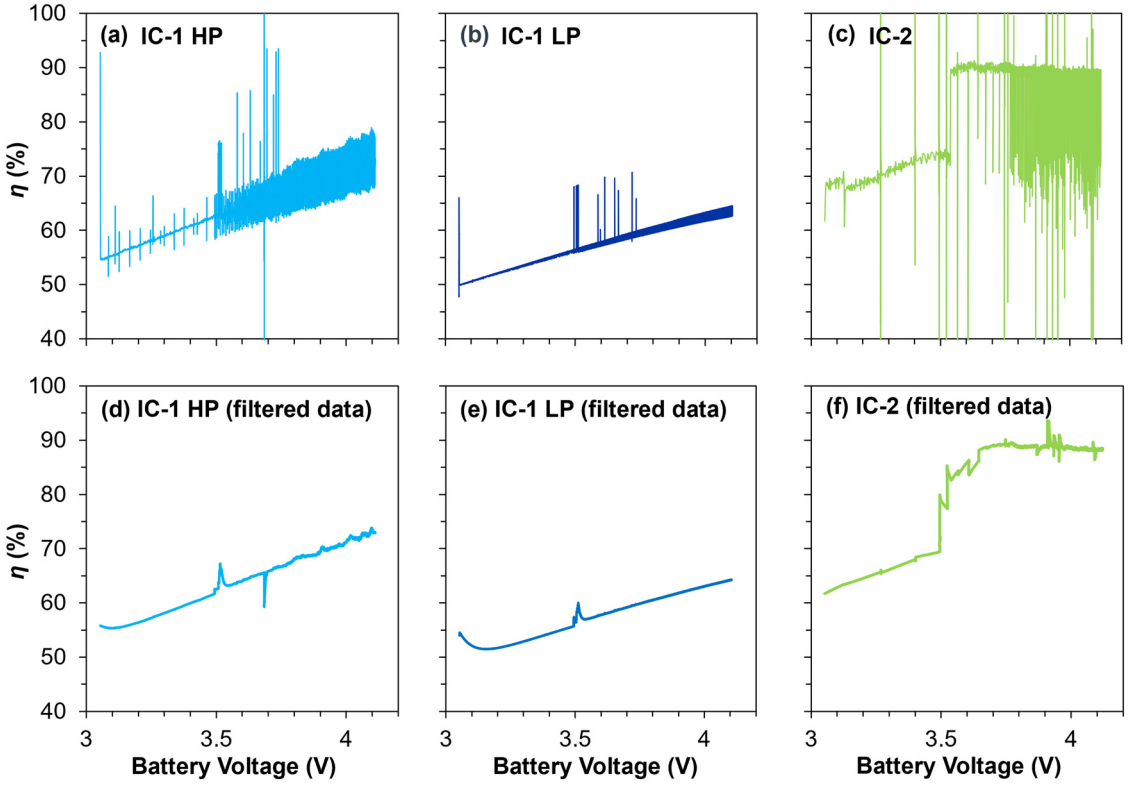

Figure 6: Dependence of η on battery voltage during charging for IC-1: (a) and (d) HP mode, (b) and (e) LP mode, and (c) and (f) for IC-2. (a)–(c) show calculated raw data and (d)–(f) show filtered data excluding artefact noise.

3.3 TM-3

Figure 7 shows the results of TM-3 where the input power to the PMICs was provided by actual PV cells under illumination. In the full range of the incident light intensity (up to 3,500 lux), Harvester-1 delivered higher input power to the PMICs than Harvester-2 when connected to IC-1 HP mode and IC-2 (Figure 7(c) and (d)). This could be expected to some extent from the manufacturer's data (Table 2). However, when connected to IC-1 LP mode, both the PV cells exhibited almost the same energy harvesting capability. It indicates that the PMICs influenced the entire energy harvesting capabilities already starting from the harvester's input side. Such an influence became even more obvious and dominant on the output side when the electricity flowed into batteries. For instance, at incident light intensities lower than 200 lux, Harvester-1 (organic PV) connected to IC-1 always outperformed Harvester-2 (amorphous silicon) connected to IC-1 for both the HP and LP modes in terms of η values (Figure 7(a) and (b)). The advantage of using Harvester-1 over Harvester-2 could reach up to 200–300%, much larger than that shown in the manufacturers' datasheets (Table 2), given that the same IC-1 was connected. When the incident light was stronger than 200 lux, the difference caused by the PV cells in the IC-1 energy harvesting systems became almost negligible despite the fact that Harvester-2 started to outperform Harvester-1 in the systems when the light intensities were over 2,000 lux.

Nevertheless, the advantage of Harvester-1 vanished, or alternatively the performance of Harvester-2 was boosted to the same level as that of Harvester-1, when IC-2 was used instead of IC-1. In such cases, both the systems (Harvester-1 + IC-2 and Harvester-2 + IC-2) were able to deliver stable charging efficiencies of approximately 80% across the entire

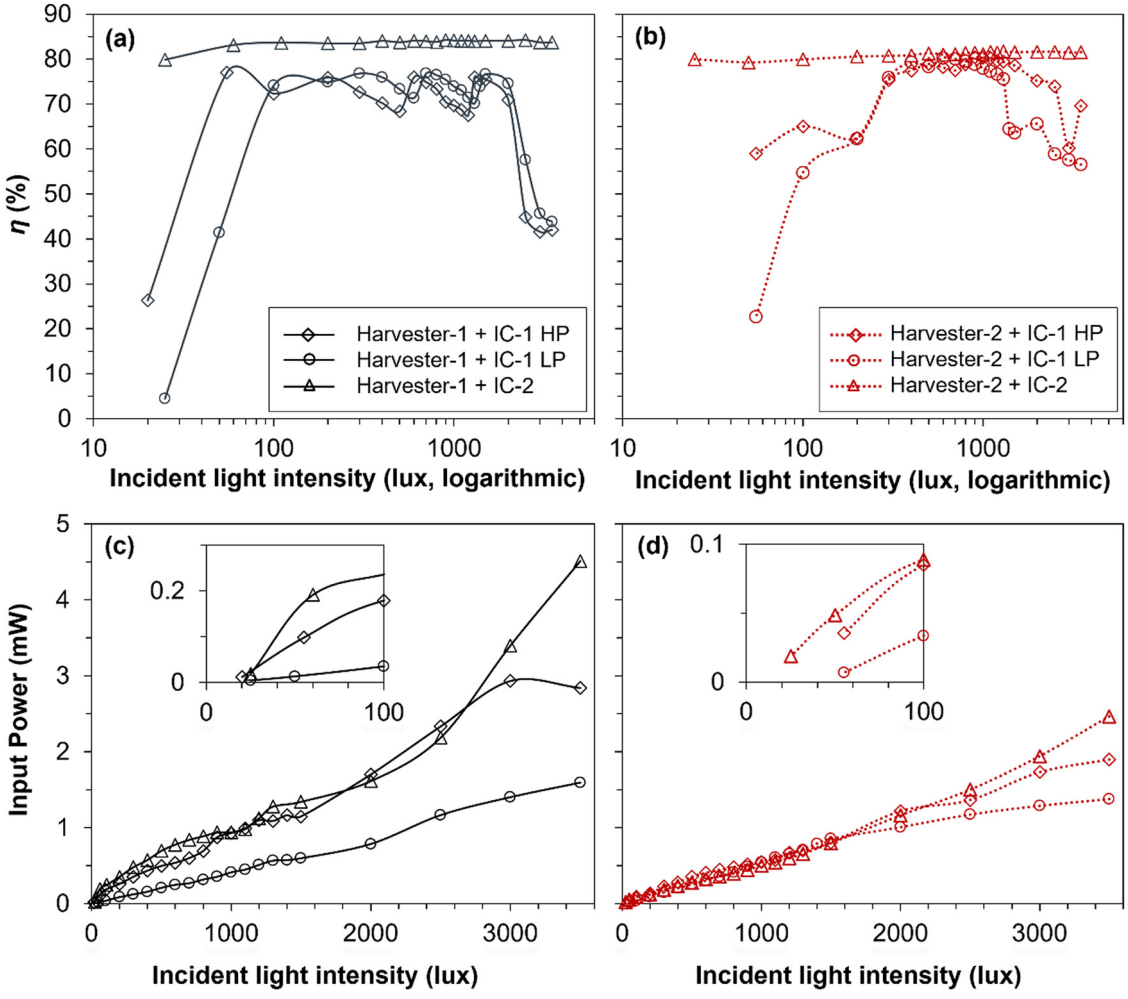

Figure 7: Dependence of η (a) and (b) and input power (c) and (d) on incident light intensity for different combinations of PV cells and PMICs. The insets of (c) and (d) show close-ups for dependence of input power on incident light intensity of <100 lux. The input power was provided to the PMIC by the PV cell exposed to indoor light. The results were obtained at a simulated battery voltage of 3.5 V.

range of the tested light intensities (Figure 7(a) and (b)). Such η values were generally higher than those delivered by the IC-1 systems regardless of which PV cell was used.

In summary, the results of TM-3 suggest that the efficiency of IC-2 across the entire range of input light intensity was generally higher and more consistent compared to that delivered by the IC-1 systems, regardless of the type of the PV cell used.

3.4 Charging a real battery under real office lighting conditions

By analyzing all results from TM-1, TM-2, and TM-3, it can be clearly seen that IC-2 performed better than IC-1 given the same input settings. To demonstrate the importance of properly selecting both the harvesters and PMICs as an overall system, an actual 500 mAh Li-ion battery at 3.7 V was finally connected to the systems to replace the battery simulator used in TM-1, TM-2, and TM-3. The battery was charged under an office lighting condition of 750–800 lux with a color temperature of about 4,300 K and the data were collected for a period of 1 min for each measurement (the same as that in TM-3).

Figure 8 provides information of the pristine output from the PV cells. Table 4 compares the performance of different energy harvesting systems with the individual performance of the components (PV cells and PMICs) stated by the manufacturers. When the PV cells were not connected to any PMIC or battery, the measured pristine output power of Harvester-1 was almost 70% more than the value provided by the manufacturer, while for Harvester-2, the measured pristine output power agreed well with the manufacturer's value. This may be because, compared to other types of PV cells, Harvester-2, which was made from amorphous silicon (Table 2), could be less influenced by the light spectrum used in this work, which was possibly different from that used to obtain the manufacturer's data (Li et al. 2015). The significant difference between Harvester-1's measured pristine output and its corresponding manufacturer's value was then likely to be caused by the different spectral conditions.

When PMICs and batteries were connected, the average output powers from the PV cells generally agreed with those shown in Figure 7(c) and (d). The η values were also consistent with the claimed PMIC efficiencies to a large extent. For the systems combining PMICs with the harvesters, surprises were found in the actual delivered power to the PMICs from the harvesters. Harvester-1 always delivered >50% higher power than that claimed in the datasheet while Harvester-2 always delivered 15–50% lower power than that claimed in the datasheet, regardless of which PMIC was connected. This fact, once again, highlights the importance of selection and matching of different components for the entire energy harvesting system where any single performance of individual components may become less determinate.

3.5 Estimation of battery life extension in real applications

In order to validate how the indoor light energy harvesting can be used to improve the battery life or to make an IoT application energy autonomous, a real application scenario of a building management system was considered. Here the sensor measured and processed the air quality, pressure, temperature, and humidity of a room. The data

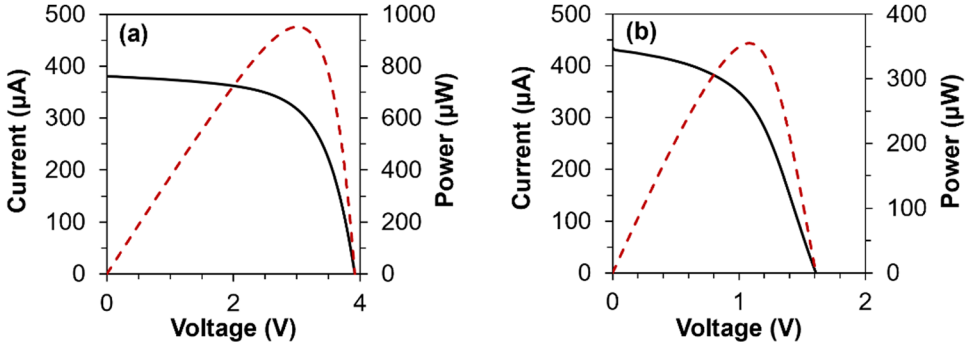

Figure 8: Dependence of current and power on voltage (I–V curve and P–V curve) measured as a pristine output directly provided by (a) Harvester-1 and (b) Harvester-2, which were not connected to any PMIC or battery, under office light of 750–800 lux intensity with a color temperature of about 4,300 K.

Table 4: Comparison of the performance of different energy harvesting systems when charging a 500 mAh Li-ion battery at 3.7 V for 1 min under indoor light

PV cell	Pristine output power from PV cell (μW)	PMIC	Output power from PV cell when connected to PMIC (μW)	Approximate PV cell output power from datasheet (μW)	Input power to battery (μW)	η (%, measured)	PMIC η in datasheet (%)
Harvester-1	950	IC-1 HP	857	550	616	72	60–80
Harvester-1	950	IC-1 LP	821	550	616	75	60–80
Harvester-2	355	IC-1 HP	189	330	109	58	60–80
Harvester-2	355	IC-1 LP	181	330	112	62	60–80
Harvester-1	950	IC-2	914	550	850	93	70–95
Harvester-2	355	IC-2	283	330	241	85	70–95

were transmitted to a cloud server using low-power LTE-M connectivity. By using the sensor datasheets and the Nordic Online Power Profiler for LTE web applications (Nordic Semiconductor 2023a), the total energy budget of an IoT application that uses LTE-M cellular connectivity to transmit 100 bytes of sensor data was calculated. Table 5 compares the total average current consumption of the stated IoT smart building application using the BME688 environmental sensor (Nordic Semiconductor 2023b) and nRF9160 LTE modem (Bosch Sensortec 2023) across different transmission intervals.

The gain in battery life by days was calculated under different energy harvesting configurations and data transmission intervals for the same battery by combining the outcomes of Tables 4 and 5, assuming that the light intensity and efficiency of the ICs remain fixed. Having demonstrated much higher efficiency in previous TM-1 and TM-2, IC-2 continued to show better performance in comparison to IC-1 with a much greater improvement in battery life across all the data transmission intervals, as shown in Table 6. The calculations also assumed the ambient light to be constant for 24 h per day as well as the battery's capacity to be 500 mAh, which neglected possible aging effects of both the battery and PV cell. This outcome was not unexpected and served to confirm the earlier findings in this work. Harvester 1 with both IC-1 and IC-2 configurations showed a significant improvement in battery life compared to Harvester-2. This is analogous to the findings of TM-3. These results imply that Harvester 1 is more effective in converting indoor light energy into electrical energy, underscoring the significance of careful selection of harvesters to ensure extended battery life. The results also indicate that the choice of IC-1 operating mode (HP/LP) did not affect the battery life for the selected light intensity. The finding of the Harvester-1 with IC-2 configuration being energy autonomous for longer transmission intervals is intriguing (Table 6), as this could potentially eliminate the need for battery replacements or recharging for such applications. It is worth mentioning that IC-1 in combination with Harvester-1 had the potential to achieve energy autonomy if the data transmission interval were to be extended beyond 30 min.

Table 5: Comparison of the average current consumption across different transmission intervals and required battery life for a 500 mAh Li-ion battery

Data transmission interval (minutes)	5	10	15	30
Average current for communication (μA)	322	162	109	90
Average current for sensing and processing (μA)	90	90	90	90
Average total current (μA)	412	252	199	180
Battery life (days)	60	83	105	116

Table 6: Comparison of the battery life improvement (gain of extended lifespan) by days for a 500 mAh Li-ion battery across different transmission intervals with indoor light harvesting

Data transmission interval (min)	5	10	15	30
Harvester-1, IC-1 HP	34	160	527	1,372
Harvester-1, IC-1 LP	34	160	527	1,372
Harvester-2, IC-1 HP	4	11	19	23
Harvester-2, IC-1 LP	4	11	19	23
Harvester-1, IC-2	64	864	∞	∞
Harvester-2, IC-2	9	29	51	65

4 Discussion

In principle, when the battery is charged more efficiently, less energy is wasted in the form of heat, which may further improve the efficiency of the energy harvesting system by minimizing the effect of temperature on the properties of the materials and components. Increased charging efficiency can induce improved performance and

longer battery life due to less variation in rated battery voltage and capacity. For a given input power, when the charging efficiency increases, the energy storage can be charged faster. This provides the opportunity to scale down the size of the battery, thereby reducing the overall size of the IoT system. This is a major benefit the designers should take advantage of at the IoT system's level in space-constraint applications, rather than working on improvements of separate components.

In this work, IC-2 outperformed IC-1 in every test case. The efficiency of IC-2 remained consistent across all power levels (10 µW–3 mW), whereas IC-1 efficiency dropped drastically at higher input power levels. The most prominent factor for this behavior could be the design architecture of the conversion circuit. In IC-1, the multi-stage, ratio-reconfigurable SC converters, as has been discussed in Section 1.3, aim to improve the conversion efficiency by offering multiple optimum voltage conversion ratios via building cascading stages. However, when the input source and the output battery voltage dynamically vary during the energy harvesting process, it could be challenging to maintain an optimum voltage ratio. In addition, only a limited number of optimum ratios could be practically implemented because additional stages could lead to an increase in loss and then further decrease the overall efficiency. Therefore, the actual voltage ratio deviated from the real-time optimum values and resulted in an increased charge redistribution energy loss (P_{CRL}) through the capacitor which is described by equation (2).

$$P_{\mathrm{CRL}} = \frac{1}{2}C(\Delta V)^2, \tag{2}$$

where C is the equivalent capacitance and ΔV is the voltage difference between the input and output ends.

In comparison, the IN boost converter in IC-2 controlled the voltage ratios more effectively in a dynamic working environment. Its inherent adaptability enabled it to handle fluctuations of input and output voltages during the energy harvesting process. This was achieved by precisely adjusting the duty cycle of the energy flow regulation in real time, which could probably only be viable with an inductor. IC-2's architecture stored energy in magnetic fields, which resulted in lower losses and higher efficiency compared to the charge transfer process dominated by the parasitic resistance of the capacitors in IC-1's architecture. Compared to off-chip inductors, the parasitic resistance of the on-chip capacitors could limit the maximum power handling capability and reduce the overall efficiency of the converter (de Souza et al. 2021). The key factors that determine the overall efficiency of the DC–DC conversion circuit are listed as follows (Forouzesh et al. 2017, Sivakumar et al. 2016):

a) Switching frequency: Higher switching frequencies can result in higher switching losses within the transistors and hence the switching frequency should be optimized for system requirements.
b) Boost conversion ratio: Ratio of the output voltage to the input voltage is the conversion ratio of a DC–DC converter. When the difference between the input and output voltages is high, power losses will also be high due to the resistance of the switching components and passive elements.
c) Power switch: Power switch is used to control and regulate the power delivered to the load. Its switching frequency and resistance determine the efficiency and output voltage of the DC–DC converter and hence it should be optimized for the specific requirements of the energy harvesting system.
d) Inductor and capacitor values: The values of the inductor and capacitor in the boost converter circuit impact the efficiency and performance of the converter. These values should be chosen carefully to achieve the desired system size, performance, and efficiency of the converter.
e) Impedance matching: Impedance matching can be achieved in two ways. First, the input impedance of the DC–DC converter should be matched to the output impedance of the harvester. Second, the impedance of the load should be matched to the impedance of the converter's output. These matching requirements should be carefully considered using passive components and different algorithms to maximize the efficiency by reducing the losses of the converter.

Regardless of the selected IC, Harvester-1 (OPV) yielded better output power under indoor lighting conditions compared to Harvester-2 (a-Si). Hence, selection of the right energy harvester is also a crucial factor which determines the overall efficiency of the system. Indoor light harvesters have a limited range of sensitivity to different wavelengths of light. They are typically designed to work under artificial light sources, such as LED, fluorescence, and incandescent lamps, and thus exhibit a narrow spectral response similar to that of the light sources (Muhammad et al. 2021). OPV cells are known to have a better performance under low-light conditions and can generate electricity from a much wider spectrum of indoor light than a-Si type cells (Xie et al. 2021). The operational voltage and current ratings of the selected harvesters should match the input ratings of the conversion circuit. If there is any mismatch, it can negatively impact the rated efficiency, actual delivered power level, and even safety of the conversion circuit.

Achieving high efficiency over a wide range of battery voltages is vital for optimal performance. This is

particularly important for Li-ion batteries, which exhibit a relatively flat voltage area across the battery's SOC range. The flat area voltage level is dependent on the exact chemistry of the selected battery. Hence, a well-designed PMIC should provide consistent, high efficiency across a wide range of battery voltages, covering the characteristics of the battery chemistry families.

Undoubtedly, in addition to the internal contributions from the systems, the position of the energy harvesting systems also plays an essential role in practice. To receive necessary energy, the harvesters and thus the systems should be placed as close to the light source as possible. Shadowing by surrounding objects should be eliminated. The orientation of the harvesters should directly face toward the light source and the angle of incident light should be optimized. The system designers should carefully assess the harvester sizes and ratings so that they fit within the space and weight constraints for certain use case.

Effective approaches for design and selection of future PMICs for IoT applications powered by indoor light energy harvesting need an essential, thorough analysis of the key parameters associated with the PMICs. For this scenario, the key parameters that IoT system-level designers should pay attention to are listed as follows.

i. **Measured efficiency.** This parameter refers to the measured boost efficiency over required input and output voltage range of the PMIC.
ii. **Cold startup condition.** This rating refers to the minimum input voltage or power that should be supplied to the PMIC to wake it up from the idle state to the activated state of the DC–DC boost conversion.
iii. **Power ratings and input range.** These ratings refer to the maximum and minimum limits of voltage, current, and power inputs that a PMIC is capable of handling.
iv. **Overcharge and over-discharge protection.** This rating refers to the presence of an internal protection circuitry to protect the battery from being overly charged or discharged.
v. **MPPT.** This feature tracks the varying input power conditions and finds the optimum point to harness and thus maximizes the power from the harvester.
vi. **Ease of integration and cost.** Important factors regarding the integration of the PMIC into the entire system include physical size, additional passive components, shape, and cost of the PMIC.

5 Conclusion and perspectives

This work has evaluated the system-level performance of indoor light energy harvesting systems integrating different types of PV cells, boost converters working on two distinct mechanisms, and a Li-ion battery. The systems were built using all-commercial components. Despite superior individual performance, results suggest that the IN boost converter unambiguously outperforms the SC counterpart in terms of battery charging efficiency when integrated into such ultralow-power indoor light harvesting systems. Detailed reasons for the IN boost converter's superior performance have been discussed. Despite the fact that an SC boost converter offers more space saving for the entire IoT system, its inferior battery charging performance in the context of connection to harvesters and batteries diminishes this good reason for choosing it to build the PMIC for practical indoor light energy harvesting systems.

By carefully choosing the energy harvesting component (e.g., using OPV cells) and then pairing it with the IN-type boost converter, IoT sensing systems powered by ambient indoor light energy sources may reach an infinite self-sufficiency under properly considered data acquisition and transmission intervals. Mismatching the harvesting and power management components, on the contrary, would put the superior performance of individual components in vain when working in a system, despite all the apparently compatible characteristic on paper.

IoT system designers should consider compromising the compactness of the PMIC by choosing the IN boost conversion in order to reach superior energy harvesting and better charging performance. The negative effect caused by the relatively bulky IN PMIC may be compensated by a much smaller battery size due to better charging efficiencies and thus shorter charging times which promote the efficient use of the limited energy budget for IoT systems.

Acknowledgements: The authors thank Joni Nyman and Olli Närhi for their constructive comments and discussions on this work.

Funding information: This work was funded by the University of Oulu, Nordic Semiconductor Oy, and the Riitta ja Jorma J. Takanen Foundation.

Author contributions: All authors have accepted responsibility for the entire content of this manuscript and consented to its submission to the journal, reviewed all the results and approved the final version of the manuscript. TH, ML and YB designed the experiments, and TH and EV carried them out. TH analysed the results and prepared the manuscript with contributions from all co-authors. YB supervised the entire research work.

Conflict of interest: Authors state no conflict of interest.

Data availability statement: The datasets generated during and/or analysed during the current study are available in the IEEEDataPort repository, DOI: 10.21227/v5zz-3414.

References

Akan O. B., Cetinkaya O., Koca C., and Ozger M. (2018). "Internet of hybrid energy harvesting things," *IEEE Internet Things J.*, vol. 5, no. 2, pp. 736–746. doi: 10.1109/JIOT.2017.2742663.

Al-Obaidi K. M., Hossain M., Alduais N. A. M., Al-Duais H. S., Omrany H., and Ghaffarianhoseini A. (2022). "A review of using IoT for energy efficient buildings and cities: A built environment perspective," *Energies*, vol. 15, no. 16, p. 5991. doi: 10.3390/en15165991.

Bai Y., Jantunen H., and Juuti J. (2018). "Energy harvesting research: The road from single source to multisource," *Adv. Mater*, vol. 30, no. 34, p. 1707271. doi: 10.1002/adma.201707271.

Bosch Sensortec. "BME688: Environmental sensing with Artificial Intelligence." https://www.boschsensortec.com/media/boschsensortec/downloads/datasheets/bst-bme688-ds000.pdf. Accessed on Nov. 24, 2023.

Brown T. M., Brainard G. C., Cajochen C., Czeisler C. A., Hanifin J. P., Lockley S. W., et al. (2022). "Recommendations for daytime, evening, and nighttime indoor light exposure to best support physiology, sleep, and wakefulness in healthy adults," *PLoS Biol*, vol. 20, no. 3, p. e3001571. doi: 10.1371/journal.pbio.3001571.

Chong Y.-W., Ismail W., Ko K., and Lee C.-Y. (2019). "Energy harvesting for wearable devices: A review," *IEEE Sens. J.*, vol. 19, no. 20, pp. 9047–9062. doi: 10.1109/JSEN.2019.2925638.

de Souza A. F., Tofoli F. L., and Ribeiro E. R. (2021). "Switched capacitor DC–DC converters: A survey on the main topologies, design characteristics, and applications," *Energies*, vol. 14, no. 8, p. 2231. doi: 10.3390/en14082231.

Dracula. "Organic PV cell datasheet." https://dracula-technologies.com/wp-content/uploads/2021/03/Demokit6-Datasheet.pdf. Accessed on Feb. 14, 2023.

Forouzesh M., Siwakoti Y. P., Gorji S. A., Blaabjerg F., and Lehman B. (2017). "Step-up DC–DC converters: A comprehensive review of voltage-boosting techniques, topologies, and applications," *IEEE Trans. Power Electron.*, vol. 32, no. 12, pp. 9143–9178. doi: 10.1109/TPEL.2017.2652318.

Jung W., Oh S., Bang S., Lee Y., Sylvester D., and Blaauw D. (2014). "23.3 A 3nW fully integrated energy harvester based on self-oscillating switched-capacitor DC–DC converter," *In 2014 IEEE International Solid-State Circuits Conference Digest of Technical Papers (ISSCC)*, pp. 398–399. doi: 10.1109/ISSCC.2014.6757486.

Kozalakis K., Sofianidis I., Konstantakos V., Siozios K., and Siskos S. (2021). "73.5 uW indoor-outdoor light harvesting system with global maximum power point tracking," *J. Low. Power Electron. Appl.*, vol. 11, no. 1, p. 10. doi: 10.3390/jlpea11010010.

Lee I., Lim W., Teran A., Phillips J., Sylvester D., and Blaauw D. (2016). "21.4 A >78%-efficient light harvester over 100-to-100klux with reconfigurable PV-cell network and MPPT circuit," *In 2016 IEEE International Solid-State Circuits Conference (ISSCC)*, pp. 370–371. doi: 10.1109/ISSCC.2016.7418061.

Li Y., Grabham N. J., Beeby S. P., and Tudor M. J. (2015). "The effect of the type of illumination on the energy harvesting performance of solar cells," *Sol. Energy*, vol. 111, pp. 21–29. doi: 10.1016/j.solener.2014.10.024.

Lin J., Yu W., Zhang N., Yang X., Zhang H., and Zhao W. (2017). "A Survey on Internet of Things: Architecture, enabling technologies, security and privacy, and applications," *IEEE Internet Things J.*, vol. 4, no. 5, pp. 1125–1142. doi: 10.1109/JIOT.2017.2683200.

Masek P., Stusek M., Zeman K., Hosek J., Mikhaylov K., Andreev S., et al. (2018) "Tailoring NB-IoT for mass market applications: A mobile operator's perspective," *In 2018 IEEE Globecom Workshops (GC Wkshps)*, pp. 1–7. doi: 10.1109/GLOCOMW.2018.8644487.

Mathews I., Kantareddy S. N., Buonassisi T., and Peters I. M. (2019). "Technology and market perspective for indoor photovoltaic cells," *Joule*, vol. 3, no. 6, pp. 1415–1426. doi: 10.1016/j.joule.2019.03.026.

Muhammad J., Kim S., and Lim D. C. (2021). "Indoor organic photovoltaics for self-sustaining IoT devices: Progress, challenges and practicalization," *ChemSusChem*, vol. 14, no. 17, pp. 3449–3474. doi: 10.1002/cssc.202100981.

Nexperia. "Electronic shelf label (ESL)." https://www.nowi-energy.com/electronic-shelf-label-esl/. Accessed on Feb. 10, 2023.

Nordic Semiconductor. "Nowi Powered Energy Autonomous Nordic Thingy:91 Platform." https://devzone.nordicsemi.com/nordic/nordic-blog/b/blog/posts/nowi-powered-energy-autonomous-nordic-thingy-91-platform. Accessed on Oct. 07, 2021.

Nordic Semiconductor. "Online Power Profiler for LTE." https://devzone.nordicsemi.com/power/w/opp/3/online-power-profiler-for-lte. Accessed on Nov. 24, 2023a.

Nordic Semiconductor. "nRF9160 Low power SiP with integrated LTE-M/NB-IoT modem and GNSS." https://infocenter.nordicsemi.com/pdf/nRF9160_PS_v2.1.pdf. Accessed on Nov. 24, 2023b.

PowerFilm Solar. https://www.powerfilmsolar.com/products/electronic-component-solar-panels/indoor-light-series/ll200-24-37. Accessed on Feb. 14, 2023.

Qiu Y., van Liempd C., het Veld B. O., Blanken P. G., and van Hoof C. (2011). "5μW-to-10mW input power range inductive boost converter for indoor photovoltaic energy harvesting with integrated maximum power point tracking algorithm," *In 2011 IEEE International Solid-State Circuits Conference*, pp. 118–120. doi: 10.1109/ISSCC.2011.5746245.

Seeman M. D., Ng V. W., Le H.-P., John M., Alon E., and Sanders S. R. (2010). "A comparative analysis of switched capacitor and inductor-based DC–DC conversion technologies," *In 2010 IEEE 12th Workshop on Control and Modeling for Power Electronics (COMPEL)*. doi: 10.1109/COMPEL.2010.5562407.

Sivakumar S., Sathik M. J., Manoj P. S., and Sundararajan G. (2016). "An assessment on performance of DC–DC converters for renewable energy applications," *Renew. Sustain. Energy Rev.*, vol. 58, pp. 1475–1485. doi: 10.1016/j.rser.2015.12.057.

SODAQ. "TRACK Extreme." https://sodaq.com/products/track-extreme/#IP69. Accessed on Feb. 10, 2023.

Telink. "Telink & Nowi Offer Energy Harvesting for TV RCUs to Meet Surging Product Demand for Environmentally Conscious Customers." https://www.telink-semi.com/news/nowi-eco-tv-remotes/. Accessed on Feb. 10, 2023.

Xie L., Song W., Ge J., Tang B., Zhang X., Wu T., et al. (2021). "Recent progress of organic photovoltaics for indoor energy harvesting," *Nano Energy*, vol. 82, p. 105770. doi: 10.1016/j.nanoen.2021.105770.

Yoon Y., Gi H., Lee J., Cho M., Im C., Lee Y., et al. (2022). "A continuously-scalable-conversion-ratio step-up/down SC energy-harvesting interface with MPPT enabled by real-time power monitoring with frequency-mapped capacitor DAC," *IEEE Trans. Circuits Syst.*, vol. 69, no. 4, pp. 1820–1831. doi: 10.1109/TCSI.2021.3139708.

Yu G., Chew K. W. R., Sun Z. C., Tang H., and Siek L. (2015). "A 400 nW single-inductor dual-input–tri-output DC–DC buck–boost converter with maximum power point tracking for indoor photovoltaic energy harvesting," *IEEE J. Solid-State Circuits*, vol. 50, no. 11, pp. 2758–2772. doi: 10.1109/JSSC.2015.2476379.

Yu H. and Yue Q. (2012). "Indoor light energy harvesting system for energy-aware wireless sensor node," *Energy Procedia*, vol. 16, pp. 1027–1032. doi: 10.1016/j.egypro.2012.01.164.

Yue X., Kauer M., Bellanger M., Beard O., Brownlow M., Gibson D., et al. (2017). "Development of an indoor photovoltaic energy harvesting module for autonomous sensors in building air quality applications," *IEEE Internet Things J*, vol. 4, no. 6, pp. 2092–2103. doi: 10.1109/JIOT.2017.2754981.

Zanella A., Bui N., Castellani A., Vangelista L., and Zorzi M. (2014). "Internet of Things for Smart Cities," *IEEE Internet Things J*, vol. 1, no. 1, pp. 22–32. doi: 10.1109/JIOT.2014.2306328.

Zeadally S., Shaikh F. K., Talpur A., and Sheng Q. Z. (2020). Design architectures for energy harvesting in the Internet of Things. *Renew. Sustain. Energy Rev.*, vol. 128, p. 109901. doi: 10.1016/j.rser.2020.109901.